Mössbauer Spectroscopy

E. Gramowski* and M. Polaski
University of Minnesota, Minneapolis, MN, USA
(Dated: March 7, 2025)

This experiment aims to investigate the principles of Mössbauer spectroscopy using a ^{57}Co gamma ray source and an Fe_3O_4 target containing ^{57}Fe. The primary objective is to study the hyperfine interactions and energy shifts caused by the nuclear environment, including isomer shifts, quadrupole splitting, and magnetic hyperfine interactions. The experimental setup involves the ^{57}Co source attached to a linear motor, a silicon detector, an Ortec 550A single-channel analyzer (SCA), and a custom LabVIEW Program. Data will be analyzed using Doppler shift calculations to associate peaks in the Mössbauer spectrum with the energy of the incident gamma rays. From this we will draw conclusions regarding hyperfine interactions within the target material.

I. INTRODUCTION

Mössbauer spectroscopy is a powerful technique for studying the local electronic and magnetic environment of nuclei in solids. First discovered by Rudolf Mössbauer in 1958, this technique utilizes the recoil-free emission and absorption of gamma rays by atomic nuclei bound in a solid lattice. Attaching the source to a linear motor allows for the exploitation of the Doppler effect to control the energy of the emitted gamma rays. The importance of this experiment lies in its application in various scientific fields, including condensed matter physics, chemistry, and material science to study the hyperfine interactions within the atomic nuclei of a target. A notable application of Mössbauer spectroscopy is within the field of space physics. Scientists have used the technique to study the fine structure of iron-rich samples from asteroids, Earth's Moon, and Mars[1]. By using a ^{57}Co source attached to an ASA MOD K3 linear motor, we will be able to tune the energy of the gamma via the Doppler effect. The velocity of the linear motor is sent to the LabVIEW program via the NI BNC-2110 DAQ. The emitted gamma rays will undergo recoil-free absorption in a Fe_3O_4 that contains ^{57}Fe. Upon de-excitation, the target produces gamma rays via recoil-free emission which go on to interact with an Amptek XR-100CR silicon detector which subsequently produces a small pulse, the amplitude of which corresponds to the energy of the incident photon. After this signal is then amplified and passed to an Ortec 550 single-channel analyzer (SCA) which filters out any pulses outside of a select range around the desired 14 keV peak. The SCA window is calibrated to deter-

* Communicating author

mine the association between the output voltage (on the scale of 0-7 volts) with the corresponding energy of the incident photon (keV scale). The SCA then passes a signal to the LabVIEW program via the DAQ where it is associated with the velocity (and thus the emitted photon energy) of the source. It is here where we explore fundamental interactions that provide insights into oxidation states, electronic configurations, and magnetic ordering.

II. THEORY

The foundation of Mössbauer spectroscopy lies in the resonant absorption of gamma rays by nuclei without recoil. When a nuclide absorbs gamma ray energy, the emitted photon can be detected at a specific energy level. We can conceptualize the profile of gamma-rays as an average energy, E_γ. The emitted gamma rays are distributed over an energy spread that follows a Lorentzian distribution, around this average energy. By leveraging the Doppler effect, we are able to modulate the energy of these gamma-rays following $\Delta E_s = (v_0/c)E_\gamma$, where v_0 is the velocity of the source. We choose a ^{57}Co source due to its unique emission properties. Initially, the source undergoes beta decay, becoming ^{57}Fe. This ^{57}Fe is in an excited state. Upon de-excitation into the relaxed state, a gamma ray is emitted.

$$^{57}\text{Co} \rightarrow ^{57}\text{Fe}^* + \beta^+ + \nu_e \; ^{57}\text{Fe}^* \rightarrow ^{57}\text{Fe} + \gamma\,(14.4\,\text{keV}) \tag{1}$$

The choice of ^{57}Co is due to the fact that this radionuclide exclusively through electron capture into its decay product of ^{57}Fe[6]. We choose a silicon detector to detect these gamma rays due to the unique detection efficiency of the material. For photons in the mid to low keV range (1-30 keV), the photoelectric effect dominates in the silicon, meaning the photon's energy is directly transferred to a photoelectron. As the photoelectron propagates through the silicon crystal lattice, it ionizes nearby atoms, creating electron-hole pairs. The detector thus applies an electric field across the silicon. Electrons move to a positive electrode and holes to a negative electrode, creating a current pulse proportional to the energy of the gamma-ray.[4][5]

A. Isomer Shift

The key theoretical concepts include isomer shift, which is a measure of the change in nuclear charge distribution due to electron density at the nucleus. This isomer shift is calculated from the electron density in the nucleus $[\Psi(0)_s]^2$, where the s-subscript refers to the electrons in the s orbital. We find that the difference in energy due to the isomer shift is calculated as:

$$\delta E = K[\Psi(0)_s]^2 R^2 \tag{2}$$

Here, K is the nuclear constant and R is the radius of the nucleus[2].

B. Quadrupole Splitting

Quadrupole splitting occurs due to the interaction between the nuclear quadrupole moment and an asymmetric electric field gradient. This splitting can be expressed as a physical quantity:

$$Q.S. = \frac{1}{2}e^2qQ(1+\eta^2/3)^{1/2} \tag{3}$$

Here, e is the charge of the proton, η is the asymmetry parameter, and Q is the quadrupole moment of the nucleus[2].

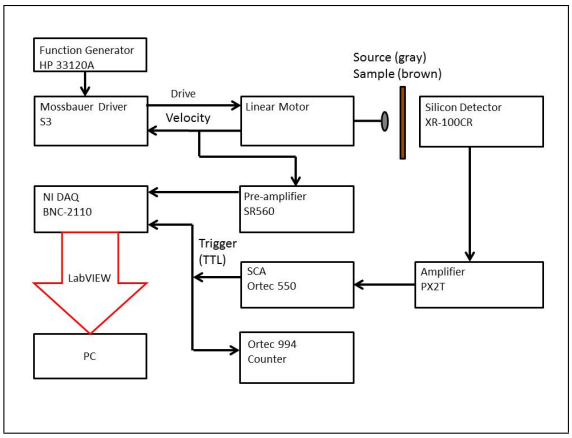

FIG. 1. Visualization of the Mössbauer apparatus, with appropriate equipment labeled[2].

C. Magnetic Splitting

Magnetic hyperfine splitting results from the interaction of the nuclear magnetic dipole moment with an internal magnetic field. This internal magnetic field can be found from the magnetic dipole moment of the nucleus, given its spin as I. This moment is defined as:

$$U_N = g_N\beta_N I \tag{4}$$

Doppler-effect modulation is used to vary the energy of gamma photons to match nuclear resonance conditions, enabling precise measurement of hyperfine interactions[2].

III. EXPERIMENTAL SETUP

We mount our ^{57}Co source, which emits 14.4 keV gamma rays, to the ASA MOD K3 linear motor. The motor is connected to the ASA S600 Mössbauer Driver via a feedback loop. The Drive component of the feedback loop is a square wave sent as a trigger signal to the linear motor and represents the voltage supplied by the driver to the motor. The Velocity component is a triangle wave. Its uniform shape indicates constant acceleration as well as even source oscillations. An HP-33120A function generator is used to supply a triangle wave reference signal at 14 Hz to the S600. The frequency is chosen due to it being close to the natural frequency of the coil springs attached to the linear motor. The Mössbauer Driver assists the motor in maintaining a constant acceleration towards the target, quickly reversing the direction, and maintaining constant acceleration away from the sample, repeating this process several times per second. This action induces the Doppler effect allowing for fine control over the energy of the source gamma ray. The Velocity component of the feedback loop is split with a BNC tee. One side goes back to the driver to complete the feedback loop, while the other goes to a Stanford Research Sys-

tems SR560 low-noise pre-amplifier. The amplified signal is sent to the computer running the custom LabVIEW program via an NI BNC-2110 DAQ and NI PCI-6036E card. Gamma rays released via the de-excitation of ^{57}Fe in the target are intercepted by an Amptek XR-100CR silicon detector. A silicon detector is used due to the material's high detection efficiency. When the high-energy photons from the target interact with the silicon, the detector emits a very small pulse, the amplitude of which is proportional to the energy of the incident photon. This pulse is amplified by the Amptek PX2T amplifier which has variable gain. We use a gain of 3.5 for data collection. The PX2T is also the power supply unit for the detector. From the PX2T, the signal is passed to the Ortec 550 single-channel amplifier (SCA). The SCA sets upper and lower limit thresholds on the energy range. This is known as windowing. If a pulse is within the window, the SCA outputs a transistor-transistor logic (TTL) pulse, if not, no pulse is emitted. This pulse is a square wave that acts as a trigger for both the digital counter (part of the LabVIEW program) and the Ortec 994 counter. The window is calibrated such that only 14.4 keV peaks are within the window. The SCA is set to its INT mode such that no external voltage is applied during data collection. From the SCA, a BNC tee splits the signal. One part is sent to the LabVIEW program via the DAQ and the other is passed to the Ortec 994 counter. The 994 is a crude way of confirming that outputs from the SCA generally represent the spectrum of ^{57}Co, however, it is very sensitive to reflection and thus is too inaccurate for any sort of data collection even with a 50Ω terminator at both the 994 and the DAQ. The 994 is used to verify the relative count rates coming out of the SCA and nothing else. The LabVIEW program then tracks the energy of the photons interacting with the silicon detector and the associated velocity of the source. From this, we are able to create a plot of energy versus velocity (proportional to the energy of the gamma-ray via the Doppler effect).

IV. PROCEDURE

The gain setting of the PX2T amplifier directly influences the position and width of the spectral peaks observed by the detector. For this experiment, a gain of 3.5 is used, as it balances signal amplification with the voltage range of the SCA (approximately 0 to 7.6 V). Excessive gain may shift the 14.4 keV peak out of the measurable range, whereas insufficient gain may result in poor peak resolution. Prior to SCA calibration, the Co-57 spectrum is examined using an Ortec EASY-MCA multi-channel analyzer (MCA). This allows for the identification of the primary spectral peaks, including the 14.4 keV peak of interest. This preliminary analysis provides essential information for setting initial SCA thresholds. We calibrate the SCA to associate output voltage of the detector with the energy of the incident gamma ray.

The SCA calibration process begins by connecting the PX2T output to the DC input of the Ortec 550 SCA. The SCA output should then be routed directly to channel B of the Ortec 994 counter, using a 50-ohm terminator to reduce reflection via impedance matching. The SCA front-panel toggle switch should be set to "WINDOW" mode, while the rear-panel toggle should be set to "EXT" for external control of the lower voltage threshold. As for the Ortec 994 counter, the display is set B and the time base is set to 10 seconds. The initial calibration involves manually adjusting the SCA lower level and window width dials to locate spectral peaks. We use the Ortec 994 counter to roughly map the Co-57 spectrum by stepping the SCA window center voltage in small increments of 0.05 volts. We record the count rates at each window center voltage and plot the data to identify the 14.4 keV peak and compare it with the expected spectrum from the MCA calibration. Areas near either side of the 14.4 keV peak have very constant noise levels. [2] Further from the peak, the signal-to-noise ratio (SNR) is less than 1. We take data with a custom LabVIEW program is used to measure counts per second as a function of window width. We vary the window width from 3.5 to 5 volts with a step size of 0.1 volts. We fit the data to a Gaussian distribution using Origin, which provides a constant background term y_0. We locate the two points where y_0 is equal to the signal and determine the center point between these two, which corresponds to the 14.4 keV peak. Once the window is centered on the 14.4 keV peak and the width is appropriately set, we connect the SCA output to the DAQ and check the ^{57}Ce spectrum to ensure only the 14.4 keV peak is visible. We set the rear panel switch on the MCA to INT for data collection. We perform a test run to ensure the apparatus is operating properly. Approximately 10,000 counts are collected and displayed on the LabVIEW interface, which should show two preliminary histograms corresponding to the detected gamma counts and a triangle wave representing the velocity profile of the oscillating source. Although meaningful absorption peaks are unlikely to be visible in such a short run, this step ensures that data is being correctly recorded, saved to the designated file location, and properly exported to a .csv file. After confirming system functionality, an extended data run is initiated, typically collecting millions of counts to ensure statistically reliable results. During these extended runs, the LabVIEW program continuously appends data to a .csv file and writes a final comprehensive data file at the end of the run, containing the complete transmission spectrum for analysis. After data collection is complete, the final .csv file is imported into Origin for further processing and analysis.

V. PROPOSED DATA ANALYSIS

Data analysis will include background subtraction to remove non-resonant gamma counts.

Peak fitting will be conducted using Gaussian or Lorentzian functions to identify hyperfine transition peaks. Parameter estimation will be performed to extract nuclear interaction parameters from the spectral shape. The final .csv file from data collection is analyzed in Origin. The file contains two columns: channel number (representing time or velocity bins) and count rate (representing detected gamma counts in each bin). In Origin, the data is plotted to form the raw transmission spectrum, which shows the characteristic Mössbauer absorption pattern, though it may initially be distorted by unwanted features such as erratic noise at the spectrum edges and a systematic quadratic trend caused by imperfections in the velocity drive system. We trim the spectrum by removing erratic data at the edges, after which the quadratic background trend is modeled and subtracted. This background removal is performed by fitting a quadratic polynomial to the sections of the spectrum that lie outside the expected peak regions, excluding the peaks themselves using Origin's masking feature. The coefficients from this quadratic fit, along with their uncertainties, are recorded and used to calculate and propagate the uncertainty in the corrected data set. With the background removed, the transmission spectrum is ready for peak fitting, which is performed using Origin's multiple peak fitting utility. The six expected peaks, corresponding to the allowed nuclear transitions in ^{57}Fe, are modeled using Lorentzian functions, reflecting the natural lineshape of Mössbauer resonances. The fitting procedure is assisted by manual placement of initial peak positions, followed by automatic refinement by the fitting algorithm. To improve the fit quality and ensure physically meaningful results, the fitting parameters can be constrained based on prior knowledge of peak spacing and width. To account for measurement uncertainties, the fitting is weighted by the propagated error column derived from the original count rates and the quadratic fit uncertainties. If noise obscures the peaks, low-pass filtering (typically over 30 to 60 channels) can be applied to improve visibility before peak fitting. Following the peak fitting, the calibrated peak positions in channel numbers must be converted into physically meaningful velocities. This calibration is performed using a known reference spectrum from a standard iron foil, for which the velocity separation between the outermost peaks is precisely 10.657 mm/s. By measuring the channel separation between these peaks, a conversion factor in mm/s per channel is obtained. This velocity calibration is then applied to the experimental spectra of all other samples. The final step is to extract key Mössbauer parameters such as the isomer shift, quadrupole splitting, and magnetic hyperfine fields by combining the calibrated peak positions using established formulas for the nuclear energy level splittings in the presence of hyperfine interactions. Each derived parameter carries an uncertainty propagated from both the peak fitting process and

the velocity calibration. Throughout the analysis, careful attention is paid to the statistical and systematic uncertainties, including those arising from counting statistics, background fitting, and calibration. The fully processed and analyzed data will provide a quantitative characterization of the sample's hyperfine interactions, which can be compared directly to literature values.

VI. SCHEDULE

The experiment will begin with a literature review, followed by the construction and calibration of the experimental setup including the MCA, SCA, and linear motor position. The data collection phase will take place over five days, with subsequent data analysis and interpretation taking up the remainder of the semester. The final report will be drafted after the completion of data analysis to document the findings and conclusions. A talk discussing methods and results will be given to a group of peers. A poster will be made and presented to peers and professionals.

[1] *Blumers, M. et al, "The miniaturized Mossbauer spectrometer MIMOS IIA: Increased sensitivity and new capability for elemental analysis", 2010*

[2] *Wick, K. Pfeifer, C. "Methods of Experimental Physics (MXP) - Moessbauer Effect Lab", 2013*

[3]

[4] *Henke, B. L., Gullikson, E. M., Davis, J. C. (1993). X-ray interactions: Photoabsorption, scattering, transmission, and reflection at E=50-30000 eV, Z=1-92. Atomic Data and Nuclear Data Tables, 54(2), 181-342. https://doi.org/10.1006/adnd.1993.1013*

[5] *Amptek. (n.d.). XR-100CR Si-PIN x-ray detector. Amptek. Retrieved March 7, 2025, from https://www.amptek.com/internal-products/xr-100cr-si-pin-x-ray-detector Mössbauer, R. L. "Nuclear Resonance Fluorescence of Gamma Radiation in Iridium.", 1958*

[6] *Chechev, V.P. Kuzmenko, N.K. "LNHB/CEA Table de Radionucléides - Co-57", 2017*

[7] *Westerdale, S. "Mossbauer Spectroscopy of 57Fe", 2010*

[8] *"The Mössbauer Effect"*

[9] *Preston, R. S. Hanna, S. S. "Mössbauer Effect in Metallic Iron", 1962*